Evaluating Least Squares Channel Estimation for Massive-MIMO OFDM

Alexander Fernandes, *260960205, alexander.fernandes@mail.mcgill.ca*

***Abstract*—The Massive-MIMO method has become popular to increase the data rates for communications based on the channel hardening phenomenon, by reducing statistical fluctuations in fading channels. However, complications occur when not considering the traditional i.i.d. Rayleigh channel. A Massive-MIMO OFDM system is tested comparing least square channel estimation for Rayleigh, Rician and Correlation channel models for Matched Filter, Zero Forcing and Minimum Mean Square Error linear detection schemes. 16, 64 and 128-QAM is compared with 64, 256 and 1024 OFDM subcarriers on Massive-MIMO channel of 50 single transmitter antennas to 50, 100, 200 and 300 receive antennas. Results show that Massive-MIMO linear detection methods have significant performance improvement at higher OFDM subcarriers but difficult to overcome performance gains in Rician and Correlation models.**

***Index Terms*—Massive MIMO, OFDM, Rayleigh, Rician, Correlation Channel, Least Squares Channel Estimation, Matched Filter, Zero Forcing, Minimum Mean Square Error.**

I. Introduction

Least squares channel estimation with linear detection has been a popularly used method for small multiple-input multiple-output (MIMO) communications channels [1]. The MIMO technique is a popular method for wireless communication to improve the reliability of the signal connection and transmit data with the goal of providing faster rates by spatially combining the signal between transmitter and receiver [2]. In addition, the digital transmission method orthogonal frequency division multiplexing (OFDM) is used in many high data rate wireless systems because of the spectrum efficiency obtained from overlap in the frequency spectrum for multiple channels [2]. But despite these efforts, new approaches are required to provide faster data transmission.

Massive-MIMO is a method that refers to using a lot more antennas for MIMO communication. Massive-MIMO benefits with increased number of antennas to offer channel hardening which reduces the statistical fluctuations in the norms of the fading channel [3]. But some problems that need to be addressed with Massive-MIMO is to use more realistic channel models to reflect the true behaviour of the radio channel [4]. With more antennas, the spatial configuration can affect the channel characteristics. Correlation-based stochastic models (CBSM) have been mainly used as a theoretical model to evaluate the performance of a Massive-MIMO system [5]. Examples of CBSM would include i.i.d. Rayleigh channel model, Rician channel model and correlation channel model [5]. Rayleigh channel model incorporates elements of i.i.d. complex gaussian variables for fast fading. Rician channel model incorporates a line-of-sight path correlation between channel coefficients [6]. The Correlation channel model contains the correlation between transmitter and receiver antennas based on the angle of azimuth and elevation [5].

With more realistic channel models, one challenging problem with Massive-MIMO is channel estimation by obtaining the channel state information (CSI). Commonly used estimation method is the least squares channel estimation (LSCE). LSCE is commonly used due to its simplicity where the channel is estimated based on a line of best fit by minimizing the sum of squared errors of the estimated channel [6].

With an estimation of the CSI, detection of the transmitted signal needs to be completed and can be more difficult for certain detection schemes in massive-MIMO as the number of channels becomes increasingly large. The Matched Filter (MF) is one of the oldest detection schemes used for recovering the transmitted signal and is optimal for maximizing the received signal from the additive white noise, known as the signal-to-noise-ratio (SNR) but fails with channel interference [1]. The Zero Forcing (ZF) detection scheme looks further by maximizing the received signal in the presence of channel interference, known as the signal-to-interference-ratio (SIR) [1]. The Minimum Mean Square Error (MMSE) detection scheme takes both methods into account by maximizing the received signal in both noise and interference, known as the signal-to-interference-plus-noise-ratio (SINR) and is theoretically the better linear detector [1].

For this project I will be replicating the work conducted by Riadi et al [7] by performing LSCE for a Massive-MIMO system using OFDM. For their study they conducted 16-QAM, 64-QAM and 128-QAM modulation with (transmit x receive) antennas of (50 x 100) and (50 x 300), but only used a i.i.d. Rayleigh channel model. To improve upon this project, three channel models will be investigated and compared using least squares channel estimation on three detection schemes. Evaluation of the Power Delay Profile and Amplitude Matrix with be observed for the three generated channels. The Mean Square Error will be used to evaluate LSCE for these three channels. Finally, BER performance will be considered for the three detection schemes used on each of the three generated Massive-MIMO channel models.

II. Body

A. Massive-MIMO Correlation-Based-Stochastic-Models

For this project three CBSM are considered: Rayleigh, Rician and Correlation used for an uplink system model. A description for each channel model is given then generated for use in sections B and C.

1) Rayleigh Channel Model

The i.i.d. Rayleigh fading channel model is the most widely adapted channel model for theoretical analysis of a massive-MIMO system and has been used as the baseline in several theoretical research studies [7]–[10]. The reason why the Rayleigh channel model is used for theoretical analysis is that it assumes no correlation between channel coefficients, making each channel from transmitter antenna to receiver antenna statistically independent to other channels [5]. The channel coefficients of this fast-fading matrix (1)

$$\boldsymbol{h}(n) = \frac{1}{\sqrt{L}} \begin{bmatrix} h_{1,1}(n) & \cdots & h_{1,Nt}(n) \\ \vdots & \ddots & \vdots \\ h_{Nr,1}(n) & \cdots & h_{Nr,Nt}(n) \end{bmatrix} \tag{1}$$

is denoted as each element $\boldsymbol{h}(n) \in C^{Nr \times Nt}$. The q^{th} receive antenna and r^{th} transmit antenna is generated for each n^{th} multipath for a total of L multipaths as (2)

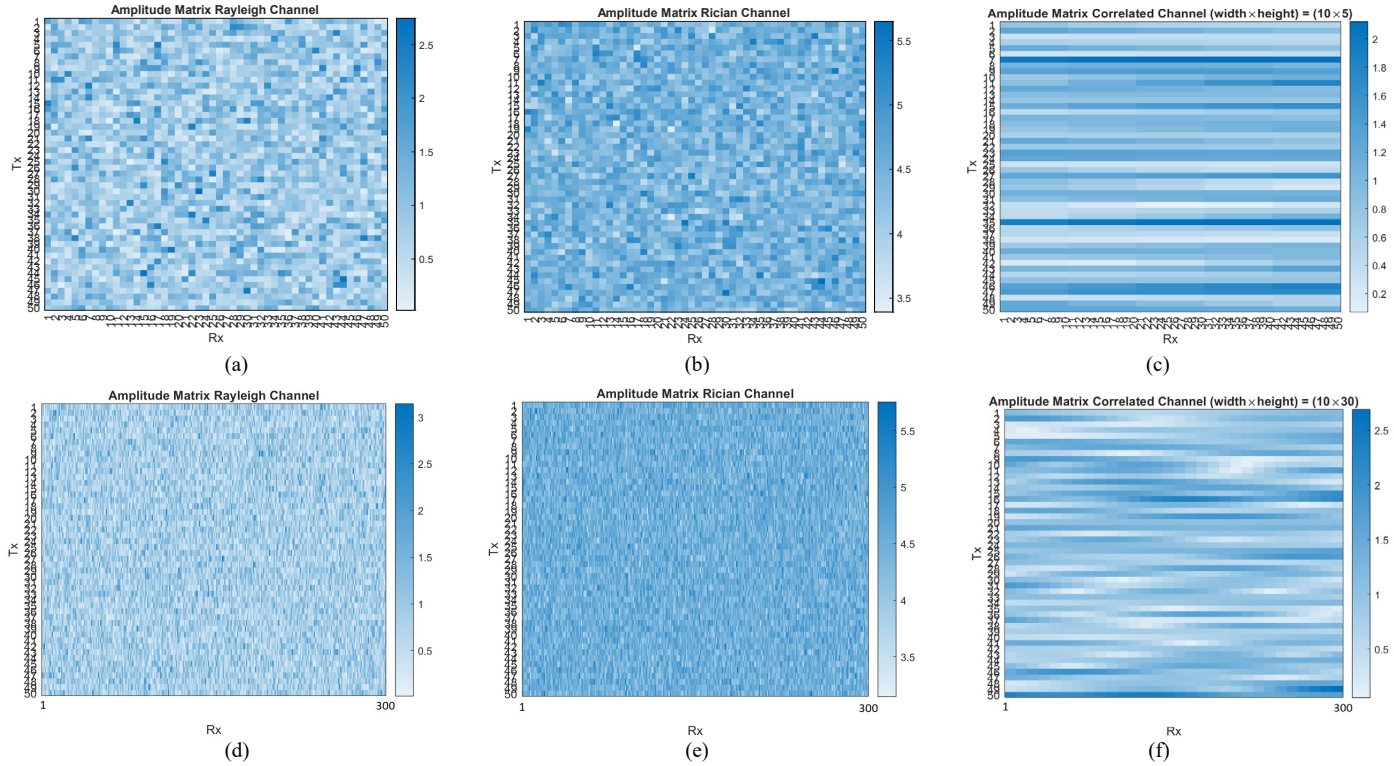

Fig. 1. Amplitude Matrix for the generated channel models Rayleigh, Rician and for (a)-(c) 50Nt, 50Nr and (d)-(f) 50Nt, 300Nr.

$$h_{q,r}(n) = \sqrt{\sigma}\big(Z_1(n) + jZ_2(n)\big) \quad (2)$$

where $Z_1(n)$ and $Z_2(n)$ are random variables generated from a normal distribution with zero mean and variance of one. The Rayleigh channel coefficient variance is chosen as $\sigma = 0.5$.

2) Rician Channel Model

The i.i.d. Rayleigh fading channel is modeled as the theoretical channel having all non-line-of-sight (NLOS) paths where as the Rician fading channel is similar but includes a line-of-sight (LOS) path [6]. With a fixed LOS, a Rician random variable would be generated similarly as in (2) but without using zero mean random variables [11]. The modification made to (2) to make it a Rician random variable using zero-mean random variables $Z_1(n)$ and $Z_2(n)$ would be generated using (3)

$$h_{q,r}(n) = \sqrt{\left(\frac{K_{ric}}{K_{ric}+1}\right)} + \sqrt{\left(\frac{1}{K_{ric}+1}\right)} \times \sqrt{\sigma}\big(Z_1(n) + jZ_2(n)\big) \quad (3)$$

where the Rician fading parameter K_{ric} is the ratio of the power in the LOS to the NLOS components where if 0 it becomes Rayleigh fading and if ∞ it becomes real and has no fading [11]. $K_{ric} = 6$ dB $= 2$ for this study to follow similar channel parameters of the I-METRA in 3GPP [12].

3) Correlation Channel Model

The Correlation fading channel is modeled to obtain the correlations between each transmitter and receiver antennas as a function of angle of azimuth (AoA) and angle of elevation (AoE) [5]. Assuming one transmitter per user equipment, each of the channel coefficients coming from one of the r^{th} transmitter (column vector in $\boldsymbol{h}$ of (1)) antennas is modeled as (4)

$$\boldsymbol{h}_r = \boldsymbol{R}_r \boldsymbol{v}_r \quad (4)$$

With $\boldsymbol{R}_r \in C^{Nr \times L}$ following L multipath steering vectors with different angles and $\boldsymbol{v}_r$ following a Rayleigh random variable

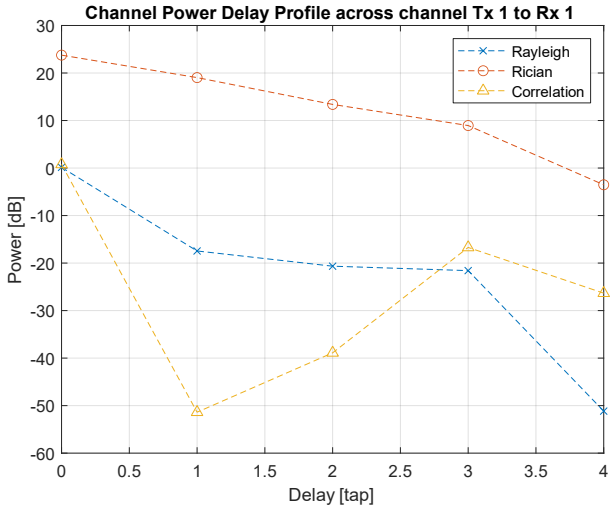

Fig. 2. Power Delay Profile of transmitter antenna 1 to receiver antenna 1 of Rayleigh, Rician and Correlation generated channel models for 50 Nt to 50 Nr antennas.

constructed as a diagonal matrix of length L. The steering matrix for each transmitter antenna is computed as (5)

$$\boldsymbol{R}_r = \big[\boldsymbol{a}(\theta_{r,1}, \phi_{r,1}), \boldsymbol{a}(\theta_{r,2}, \phi_{r,2}), \dots, \boldsymbol{a}(\theta_{r,L}, \phi_{r,L})\big] \quad (5)$$

with following a rectangular array, each i^{th} steering vector path is a function of $\theta_{r,i}$ AoA and $\phi_{r,i}$ AoE as (6)

$$\boldsymbol{a}(\theta_{r,i}, \phi_{r,i}) = vec\left\{\left[1, e^{j\left(\frac{2\pi d}{\lambda}\right)sin\theta_{r,i}}, \dots, e^{j\left(\frac{2\pi(N_r-1)d}{\lambda}\right)sin\theta_{r,i}}\right]^T \otimes \left[1, e^{j(2\pi d/\lambda)sin\phi_{r,i}}, \dots, e^{j(2\pi(N_r-1)d/\lambda)sin\phi_{r,i}}\right]\right\} \quad (6)$$

The $vec\{\cdot\}$ denotes the vectorization of a matrix operator and $\otimes$ the Kronecker product of the two steering vectors, used to multiply the AoA and AoE throughout all N_r received antennas coming from the r^{th} single transmitter antenna [13]. For this

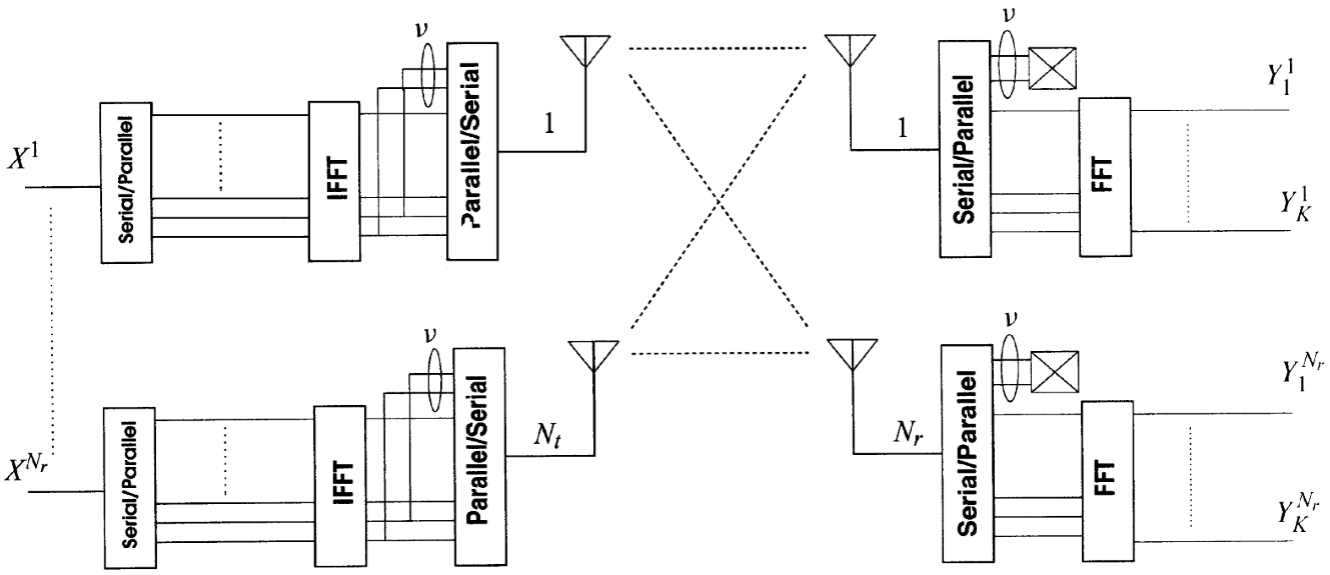

Fig. 3. System Model of MIMO-OFDM uplink transmission from Nt transmission antennas to Nr receive antennas. Figure obtained from Fig. 1 of I. Barhumi et al [14].

study, the wavelength used was $\lambda = \frac{3\times10^8}{3GHz}$ and $d = \frac{\lambda}{2}$ spacing between each antenna. The AoA $\theta_{r,i}$ was chosen as evenly spaced angles between 0 and 180° depending on r^{th} transmitter antenna and the AoE $\phi_{r,i}$ was chosen as a random uniform variable between -35° and -25° to simulate a potential massive-MIMO base station that might be placed higher above user equipment on an open wall.

4) Amplitude Channel Matrix and Power Delay Profile

The amplitude matrix (AM) is plotted as the sum of the absolute value over all L multipaths in Fig. 1 to show the correlation distribution spatially across the channel models. To show the result of generating the Rayleigh, Rician and Correlation channel models the Power Delay Profile (PDP) is obtained by taking the autocorrelation of the channel along the n multipath axis to show the power correlation of the delay in Fig. 2.

In Fig. 1, the AM of the three channels shows that the Rayleigh and Rician channels follow a random distribution of amplitudes. The Rayleigh and Correlated channel have approximately the same maximum amplitude distribution while the Rician as double maximum amplitude (6 dB). Finally in the correlated channel a clear spatial correlation can be seen between similar receive antennas (Rx direction has relatively all have the same amplitude) but no correlation occurring between transmitter antennas (along the Tx direction).

We see in Fig. 2 that for both generated channel model sizes, PDP is always larger for the Rician channel due to the $K_{ric} =$ 6 dB. This means that the LOS path is modeled to be much more prevalent in the Rician channel and seemingly non-existent in the Rayleigh and Correlation channel models. With $L = 5$ multipaths, the power of the autocorrelation follows a general decaying trend as the delay increases. This effectively represents the first path (zero delay) as the main component with the following paths (at delays greater than one) always being a lesser amplitude of the main component signal.

B. Massive-MIMO-OFDM Channel Estimation

In this section the uplink system is modeled for a Massive-MIMO-OFDM implementation. The idea is the transmit signal is encoded into the complex number of the corresponding M-QAM symbol then represented as a frequency domain signal. The inverse discrete Fourier transform is applied to convert it into a time domain signal, passes through the channel model generated in section A. Then finally the received signal is used to estimate the CSI using least squares channel estimation from pilot signals.

1) Quadrature Amplitude Modulation

Quadrature Amplitude Modulation (QAM) is used to convert the binary signal into one of M constellation points represented as a complex number in (1).

$$X = a + jb \tag{7}$$

Where $a, b \in \{\pm1, \pm3, \dots, \pm\sqrt{M}-1\}$ to encode the binary representation into the complex symbol X to be sent [2]. With a higher value of M, more data can be transmitted per symbol, however as M increases the probability of a bit error occurring also increases because there are more symbols per signal to noise ratio. Each M-QAM generated signal is normalized to maintain the same SNR-per-bit $\frac{E_b}{N_0}$ as: $\sqrt{\frac{3}{2(M-1)}\frac{E_b}{N_0}}$ [2].

2) Orthogonal Frequency Division Multiplexing

Fig. 3 shows the overall method form MIMO Orthogonal frequency division multiplexing. The benefit of this is we can break down the multiple paths by analogy as a single path OFDM transmission before describing MIMO-OFDM. OFDM is a technique that converts the frequency domain M-QAM symbol X into a time domain representation x using the Inverse Discrete Fourier Transform (IDFT) to be transmitted over the channel as a time domain signal, to be received and converted back into the complex frequency representation using the Discrete Fourier Transform (DFT). The length of the DFT is represented with having K OFDM subcarriers at different frequencies. Subcarriers represents the number of

orthogonal channels that the signal can be transmitted using the property that different frequency bands are orthogonal to each other. When transmitting an OFDM represented symbol, a cyclic prefix (CP) (represented as v in Fig. 3) is added to extend the transmitted OFDM symbol to be longer than the maximum delay of the multipath fading channel [6]. This is to ensure that the transmitted signals $\boldsymbol{x}$ properly convolves with the channel coefficients without the convolution being affect by the multiple paths.

3) Massive-MIMO Uplink System

Following Fig. 3 as reference for MIMO-OFDM obtained from Fig 1 of I. Barhumi et al [14], this Massive MIMO system is performed using uplink transmission from N_t number of single transmission antennas to a base station with N_r receive antennas. Because this is a Massive-MIMO-OFDM channel we end up with the following received signal y_q of the q^{th} receive antenna in (2).

$$y_q = \sum_{r=1}^{N_t}\left(h_{q,r}(n) * x_r(n)\right) + \gamma_q \qquad (8)$$

Where $h_{q,r}(n)$ is the time domain fading channel coefficient that is a $1 \times L$ vector (L taps) and convolved through the time domain via the $*$ operation with the transmitted signal $x_q(n)$ from the r^{th} transmit antenna denoted with n as time index [10]. AWGN γ_q is added to the q^{th} receive antenna after the convolution across all transmit antennas.

4) Least Squares Channel Estimation

Least square channel estimation (LSCE) is a commonly used and efficient method to estimate the CSI [7], [10], [14], [15]. This method of minimizing this cost function is equivalent to minimizing the mean square error (MSE) between the received signal and estimated channel applied to the send signal.

To perform channel estimation, training data symbols are used by adding in OFDM pilot symbols into the OFDM vector. The pilot signals are known to both the receiver and transmitter and the channel can be estimated by training with the pilot symbols then tested on all the other unknown transmitted OFDM signals [6]. The transmission signal is can then be represented as the combination of messages $\boldsymbol{S}_r(k)$ and pilot tones $\boldsymbol{B}_r(k)$ for the r^{th} transmitter antenna (9)

$$\boldsymbol{X}_r(k) = \boldsymbol{S}_r(k) + \boldsymbol{B}_r(k) \qquad (9)$$

The pilot symbols are then used as training data to minimize the mean square error along each subcarrier frequency. The matrix $\boldsymbol{A}(k)$ was formulated from I. Barhumi et al [14] being $K \times LN_t$ dimension (for each k^{th} OFDM subcarrier). This matrix containing all incoming pilot symbols is used to minimize the formulated mean square error of the received signal and estimated channel as (10)

$$\boldsymbol{A} = [\text{diag}\{\boldsymbol{B}_1 F\}, \ldots, \text{diag}\{\boldsymbol{B}_{Nt} F\}] \qquad (10)$$

with F being the DFT matrix, but only the first L columns are used because knowledge of the number of multipaths is assumed.

When performing LSCE formulation of the cost function should be based on the combination of the q^{th} received antenna being trained with pilot sequences of all Nt transmission antennas and assumed over one OFDM symbol where $\text{diag}\{\boldsymbol{B}_r(k)\}$ diagonalizes the r^{th} transmitted pilot symbol across all Nt transmitted antennas for the q^{th} received antenna. The cost function for LSCE is formulated as (11)

$$J\left(\widehat{\boldsymbol{H}}_q(k)\right) = \left\|\boldsymbol{Y}_q(k) - \widehat{\boldsymbol{H}}_q(k)\boldsymbol{A}(k)\right\|^2 \qquad (11)$$

The capitalization of the bold matrices denotes LSCE being performed in the frequency domain for each k^{th} OFDM. $\boldsymbol{B}(k)$ is a vector containing the OFDM pilot sequences. Where $\widehat{\boldsymbol{H}}_{LS}(k)$ is estimated as the frequency domain representation by the k^{th} OFDM subcarrier. The LS channel estimate is solved in [14] as (12)

$$\widehat{\boldsymbol{H}}_q(k) = \boldsymbol{A}^{+}(k)\boldsymbol{Y}_q(k) \qquad (12)$$

the result in being the pseudo-inverse of $\boldsymbol{A}(k)^{+} = \left(\boldsymbol{A}(k)^H \boldsymbol{A}(k)\right)^{-1}\boldsymbol{A}^H(k)$. The interesting property of the pseudo-inverse is that effectively every $\text{diag}\{\boldsymbol{B}_r(k)\}$ transmitted element is being squared, inversed, and multiplied by the conjugate transpose. This can be thought of as multiplying weighted sum of elements in $\boldsymbol{A}^{+}\boldsymbol{Y}$ as $\frac{\sum a_l^* y_l}{\sum |a_l^2|}$.

5) Measured Mean Square Error of Channel Estimation

Fig. 4 shows the result of the measured MSE for LSCE for the three generated channel models at $(N_r = 50, N_t = 50)$ and $(N_r = 300, N_t = 50)$. We see that the MSE is slightly smaller as the number of receive antennas is increased. We also see that

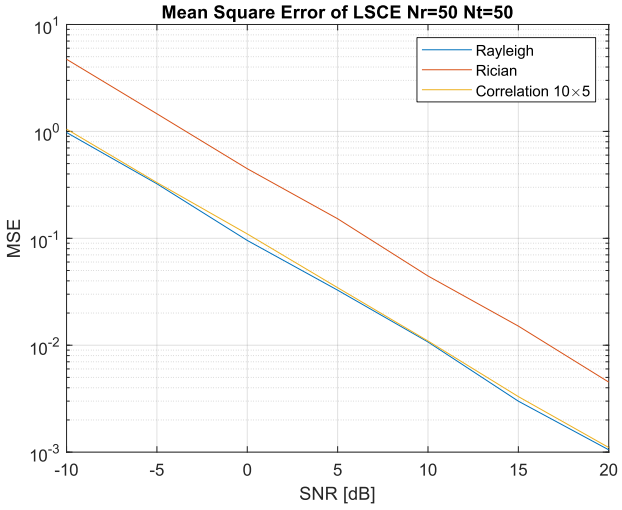

Fig. 4 Mean Square Error of Least Squares Channel Estimation for Rayleigh, Rician and Correlation channels on 128-QAM with 1024 OFDM subcarriers using (a) 50 Nt to 50 Nr antennas and (b) 50 Nt to 300 Nr antennas.

TABLE I
MSE OF LSCE FOR 50 NT TO 50 NR AT SNR 5 DB

OFDM Subcarriers	M-QAM	Rayleigh	Rician	Correlation (10×5)
64	16	6.7214 E-2	3.1281 E-0	2.9421 E-1
64	64	6.6109 E-2	3.1555 E-0	3.0126 E-1
64	128	6.8819 E-2	3.5922 E-0	2.7155 E-1
256	16	7.0594 E-2	1.5988 E-0	1.6424 E-1
256	64	6.5497 E-2	2.1385 E-0	1.9336 E-1
256	128	6.7735 E-2	1.8423 E-0	1.7594 E-1
1024	16	3.0952 E-2	1.0879 E-1	3.2287 E-2
1024	64	3.1920 E-2	1.2351 E-1	3.1625 E-2
1024	128	3.2731 E-2	1.5241 E-1	3.4534 E-2

TABLE II
MSE OF LSCE FOR 50 NT TO 300 NR AT SNR 5 DB

OFDM Subcarriers	M-QAM	Rayleigh	Rician	Correlation (10×30)
64	16	3.6476 E-2	3.5693 E-0	1.6908 E-1
64	64	3.5966 E-2	3.2485 E-0	1.7413 E-1
64	128	3.6624 E-2	3.8035 E-0	1.5498 E-1
256	16	4.1148 E-2	2.0428 E-0	1.2068 E-1
256	64	4.0827 E-2	2.1208 E-0	9.0875 E-2
256	128	4.0421 E-2	1.8677 E-0	9.8512 E-2
1024	16	2.2240 E-2	9.1005 E-2	2.2708 E-2
1024	64	2.2208 E-2	9.2174 E-2	2.1836 E-2
1024	128	2.2230 E-2	9.0250 E-2	2.3469 E-2

the Rayleigh and Correlation channels have very similar MSE while the Rayleigh channel consistently has higher MSE but with the same slope. This can be understood because the MSE of LSCE is inversely proportional to the signal to noise ratio and the Rician channel was generated with a power ratio of 6 dB LOS to NLOS.

Table I and II show the detailed results of the MSE for the LSCE for $(N_r = 50, N_t = 50)$ and $(N_r = 300, N_t = 50)$ at a low SNR of 5 dB. One interesting observation that is made is the size of the M-QAM symbol does not seem to affect the performance of the massive-MIMO LSCE very much. Across all channels we notice that many OFDM subcarriers at $K = 1024$ performs significantly better than 64 and 256 subcarriers. One possibility for this could be the increased number of pilot symbols for the single OFDM symbol used to train the LSCE, showing that the benefit of higher OFDM allows for more training symbols in single shot OFDM training implementation.

As N_r increases from 50 to 300, performance in the MSE improves throughout all Rayleigh and Correlation channels, but not all Rician channels. The Rician channel only improves for 1024 OFDM subcarriers. This is interesting to note because the bandwidth plays an important factor when minimizing the LSCE for highly correlated channels.

C. Massive-MIMO Linear Detection

The goal of Massive-MIMO Detection is to use the estimated CSI to decode the original transmitted message. In Fig. 5 obtained from Fig. 19 of S. Yang and L. Hanzo [1], shows the method for linear detection where the goal is to determine T to obtain the estimated transmitted send message as (13)

$$\widehat{\boldsymbol{S}} = \boldsymbol{TY} \tag{13}$$

where $\widehat{\boldsymbol{S}}$ for our study is the frequency domain transmit signal from all N_t transmitter antennas using N_r $\boldsymbol{Y}$ receiver

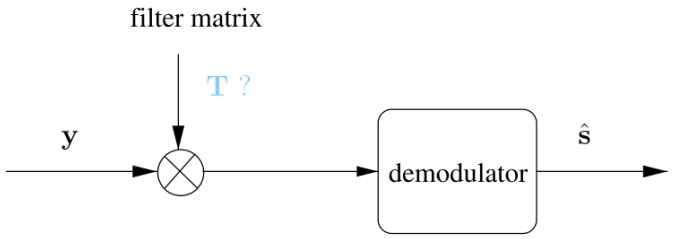

Fig. 5. Conceptual illustration of linear MIMO detection obtained from Fig. 19 of S. Yang and L. Hanzo [1].

antennas. The advantage of Massive-MIMO systems is the higher SNR occurring from the combination of receiver antennas without bandwidth trade-off [16].

1) Matched Filter Detection

The Matched Filter (MF) detection scheme is the simplest linear detection scheme and has the lowest computational complexity [1].

$$\boldsymbol{T}_{MF} = \widehat{\boldsymbol{H}}^H \tag{14}$$

The MIMO detector is simply the complex transpose of the estimated MIMO channel. The main benefit is this was designed to maximize the output SNR with additive white gaussian noise [1]. The detection scheme solves as follows (15).

$$\widehat{\boldsymbol{S}} = \widehat{\boldsymbol{H}}^H\boldsymbol{Y} = \widehat{\boldsymbol{H}}^H\boldsymbol{HS} + \widehat{\boldsymbol{H}}^H\boldsymbol{N} \tag{15}$$

The optimal linear detection works very well when $\widehat{\boldsymbol{H}}^H = \boldsymbol{H}^{-1}$ and when $\boldsymbol{N}$ is very low (when SNR is very high). However, the MF is not very beneficial for Massive-MIMO systems having a very large SIR.

2) Zero Forcing Detection

The Zero Forcing (ZF) detection scheme is the result of assuming $\boldsymbol{N}$ is very low and involves solving $\boldsymbol{T}_{ZF}\boldsymbol{Y}$ as a system of linear equations using the Moore-Penrose pseudoinverse of the estimated channel [1] as

$$\boldsymbol{T}_{ZF} = \widehat{\boldsymbol{H}}^{+} \tag{16}$$

This effectively results in adding up the weighted sums of the elements (like the LSCE) but through maximum ratio combining of the weighted sum from the direction of the r^{th} send message (capitalization for frequency domain) to the channel coefficient in (17)

$$\widehat{\boldsymbol{S}} = \widehat{\boldsymbol{H}}^{+}\boldsymbol{Y} = \widehat{\boldsymbol{H}}^{+}\boldsymbol{HS} + \widehat{\boldsymbol{H}}^{+}\boldsymbol{N} = \frac{\sum H_r^* S_r}{\sum |H|^2} + \widehat{\boldsymbol{H}}^{+}\boldsymbol{N} \tag{17}$$

With the pseudoinverse we understand that $\widehat{\boldsymbol{H}}^{+} = \boldsymbol{H}^{-1}$ when $N_r \gg N_t$ and for this reason overcomes the SIR problem that occurs with MF detection as N_r increases.

3) Minimum Mean Square Error Detection

The Minimum Mean Square Error (MMSE) detection scheme is the result of taking the ZF linear detector one step further by trying to minimize the additive white noise (18)

$$\boldsymbol{T}_{MMSE} = \underset{\boldsymbol{T}}{\operatorname{argmin}} \|\boldsymbol{S} - \boldsymbol{TY}\|^2 \tag{18}$$

This minimization is solved in [1] as an extension of the pseudoinverse by also taking the noise as consideration in the denominator (19)

$$\boldsymbol{T}_{MMSE} = \left(\widehat{\boldsymbol{H}}^H\widehat{\boldsymbol{H}} + 2\sigma^2\boldsymbol{I}\right)^{-1}\widehat{\boldsymbol{H}}^H \tag{19}$$

For MMSE it is assumed that the additive white noise SNR exhibited in the channel is known and σ^2 is represented as the

noise power to signal ratio (inverse of the SNR). Because of this the MMSE achieves better performance to that of the ZF detector under lower SNR conditions [1].

4) Massive-MIMO Detection

This section shows the full results of the MF, ZF and MMSE detection schemes performed on the generated Rayleigh, Rician and Correlation channels using the LSCE estimate of the CSI. Fig. 6 shows the Bit Error Rate (BER) of the three

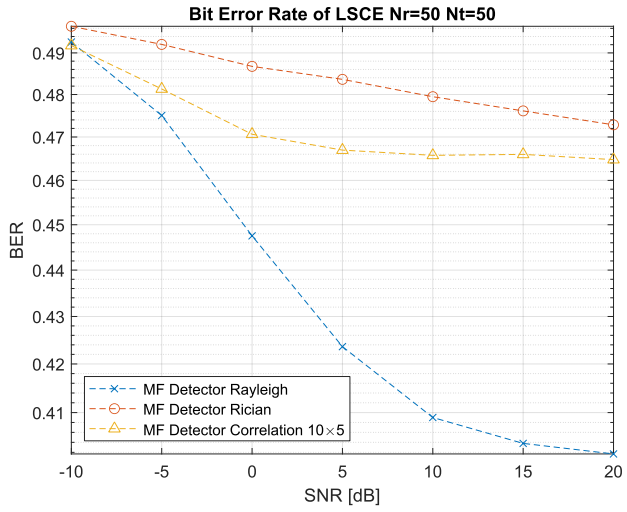

(a)

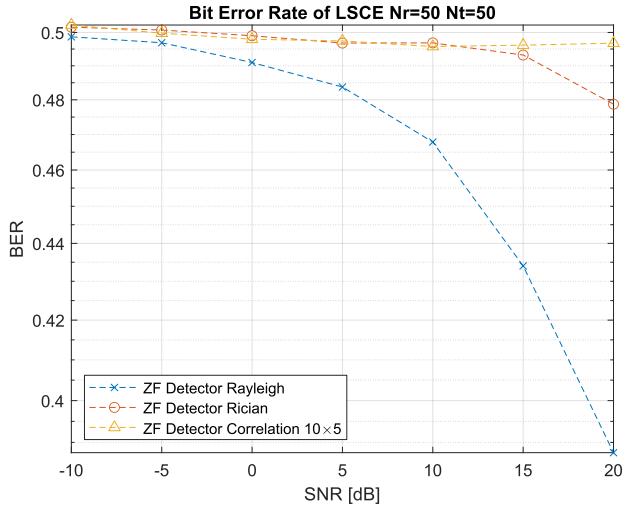

(b)

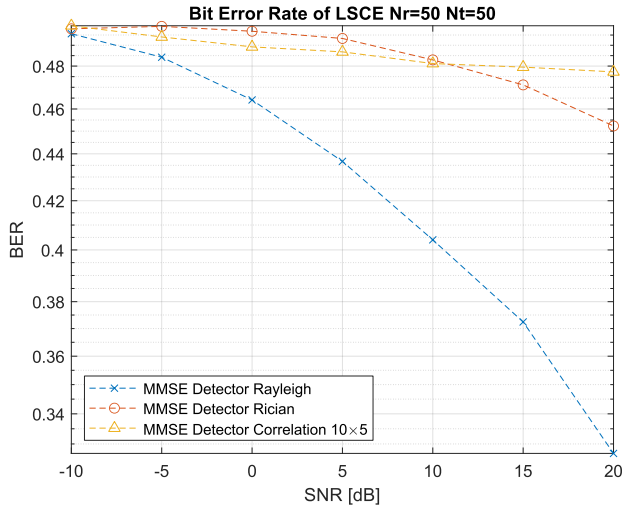

(c)

Fig. 6 Bit Error Rate of Rayleigh, Rician and Correlation channels on 50 Nt to 50 Nr, 128-QAM with 1024 OFDM subcarriers using detection method (a) Matched Filter (b) Zero Forcing (c) Minimum Mean Square Error.

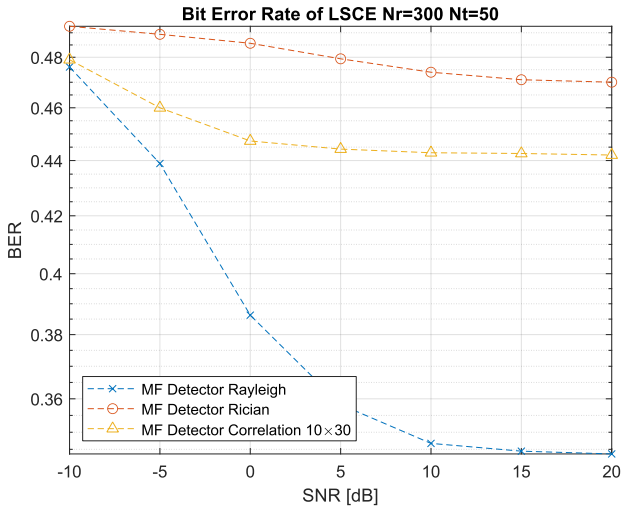

(a)

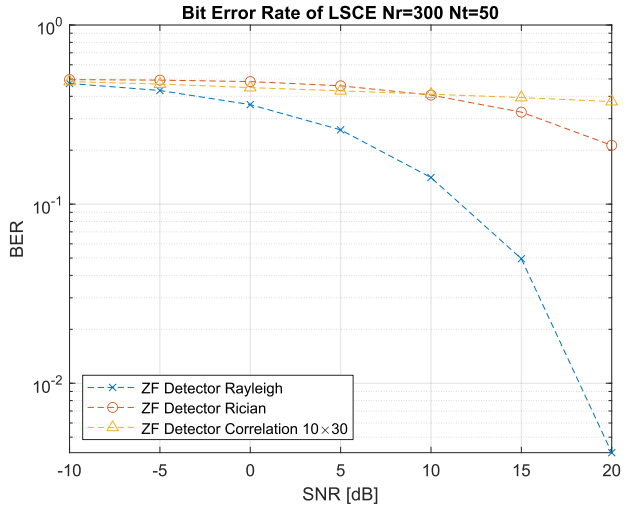

(b)

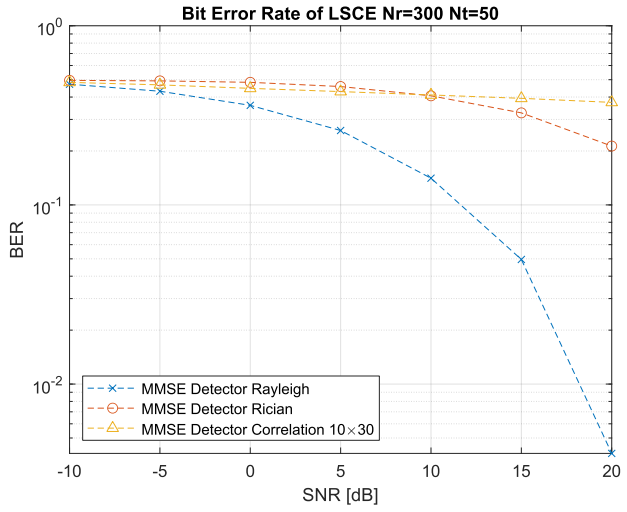

(c)

Fig. 7 Bit Error Rate of Rayleigh, Rician and Correlation channels on 50 Nt to 300 Nr, 128-QAM with 1024 OFDM subcarriers using detection method (a) Matched Filter (b) Zero Forcing (c) Minimum Mean Square Error.

TABLE III
BER FOR 50 NT TO 300 NR RAYLEIGH CHANNEL AT SNR 5 DB

OFMD Subcarriers	M-QAM	MF	ZF	MMSE
64	16	4.3938 E-1	5.0641 E-1	4.6297 E-1
64	64	4.6042 E-1	5.0208 E-1	4.7813 E-1
64	128	4.6330 E-1	4.9696 E-1	4.8161 E-1
256	16	3.6231 E-1	3.5184 E-1	3.4973 E-1
256	64	4.1716 E-1	4.0641 E-1	4.0331 E-1
256	128	4.1152 E-1	4.1634 E-1	4.1545 E-1
1024	16	3.0190 E-1	1.1686 E-1	1.1702 E-1
1024	64	3.7115 E-1	2.1217 E-1	2.1245 E-1
1024	128	3.5825 E-1	2.5990 E-1	2.6026 E-1

TABLE IV
BER FOR 50 NT TO 300 NR RICIAN CHANNEL AT SNR 5 DB

OFMD Subcarriers	M-QAM	MF	ZF	MMSE
64	16	4.9094 E-1	5.0188 E-1	4.8859 E-1
64	64	4.9031 E-1	5.0740 E-1	4.9240 E-1
64	128	4.9571 E-1	5.0920 E-1	5.0089 E-1
256	16	4.7801 E-1	4.8059 E-1	4.8023 E-1
256	64	4.9182 E-1	4.8635 E-1	4.8786 E-1
256	128	4.8734 E-1	4.8741 E-1	4.8737 E-1
1024	16	4.6448 E-1	4.2159 E-1	4.2157 E-1
1024	64	4.7560 E-1	4.5113 E-1	4.5107 E-1
1024	128	4.7940 E-1	4.5793 E-1	4.5792 E-1

TABLE V
BER FOR 50 NT TO 300 NR CORRELATION (10×30) CHANNEL AT SNR 5 DB

OFMD Subcarriers	M-QAM	MF	ZF	MMSE
64	16	4.7813 E-1	4.9906 E-1	4.8688 E-1
64	64	4.8604 E-1	5.0073 E-1	4.9156 E-1
64	128	4.8884 E-1	5.0464 E-1	4.8714 E-1
256	16	4.4082 E-1	4.6043 E-1	4.5910 E-1
256	64	4.6563 E-1	4.7375 E-1	4.7198 E-1
256	128	4.6080 E-1	4.7681 E-1	4.7435 E-1
1024	16	4.1268 E-1	3.8016 E-1	3.7935 E-1
1024	64	4.4100 E-1	4.2258 E-1	4.2216 E-1
1024	128	4.4437 E-1	4.2924 E-1	4.2912 E-1

detection schemes compared for each channel model at $(N_r = 50, N_t = 50)$. In all detection schemes we see that with many transmitter antennas to receive antennas, the performance is low. But in the MF detection scheme we see that the order of performance is decreasing from Rayleigh to Correlation to Rician (order of higher to lower SIR) which corresponds with the idea that the MF performs worse under lower SIR.

Fig. 7 shows the Bit Error Rate (BER) performance like Fig. 6 but modeled at $(N_r = 300, N_t = 50)$. The relative performance between each channel and detection method remains the same with Rician improving over Correlation channel for ZF and MMSE as SNR improves beyond SNR of 15 dB. The most notable improvement is that the performance drastically improves for ZF and MMSE but very little for MF because the MF detection scheme has trouble with the resulting channel interference for each increase in receiver antenna.

Tables III through VIII show more detail of the large number of receive antenna $(N_r = 300, N_t = 50)$ for 64, 256 and 1024 OFDM subcarriers and 16, 64 and 128 M-QAM. Tables III-V are for SNR 5 dB and Tables VI-VIII for 15 dB. The performance doesn't increase at all for all channel model and detection schemes using 64 OFDM subcarriers showing that a larger bandwidth is required for Massive-MIMO systems. This corresponds with the results of [7], [10] where 64 OFDM subcarriers Massive-MIMO

TABLE VI
BER FOR 50 NT TO 300 NR RAYLEIGH CHANNEL AT SNR 15 DB

OFMD Subcarriers	M-QAM	MF	ZF	MMSE
64	16	4.3281 E-1	4.9188 E-1	4.8141 E-1
64	64	4.5677 E-1	5.0271 E-1	4.8229 E-1
64	128	4.6438 E-1	4.9652 E-1	4.9384 E-1
256	16	3.4852 E-1	2.6309 E-1	2.6273 E-1
256	64	4.0828 E-1	3.3758 E-1	3.3708 E-1
256	128	4.0027 E-1	3.6830 E-1	3.6795 E-1
1024	16	2.8525 E-1	7.8125 E-5	7.8125 E-5
1024	64	3.6262 E-1	1.7734 E-2	1.7773 E-2
1024	128	3.4447 E-1	4.9565 E-2	4.9610 E-2

TABLE VII
BER FOR 50 NT TO 300 NR RICIAN CHANNEL AT SNR 15 DB

OFMD Subcarriers	M-QAM	MF	ZF	MMSE
64	16	4.8953 E-1	5.0250 E-1	4.7922 E-1
64	64	4.8969 E-1	5.0646 E-1	4.8542 E-1
64	128	4.9670 E-1	4.9732 E-1	4.9616 E-1
256	16	4.7266 E-1	4.0180 E-1	4.0106 E-1
256	64	4.8646 E-1	4.2990 E-1	4.2932 E-1
256	128	4.8036 E-1	4.4248 E-1	4.4181 E-1
1024	16	4.5252 E-1	1.9593 E-1	1.9600 E-1
1024	64	4.6780 E-1	2.8872 E-1	2.8879 E-1
1024	128	4.7100 E-1	3.2635 E-1	3.2644 E-1

TABLE VIII
BER FOR 50 NT TO 300 NR CORRELATION (10×30) CHANNEL AT SNR 15 DB

OFMD Subcarriers	M-QAM	MF	ZF	MMSE
64	16	4.7547 E-1	4.9391 E-1	4.9594 E-1
64	64	4.8490 E-1	5.0010 E-1	5.0438 E-1
64	128	4.8750 E-1	5.0232 E-1	4.8670 E-1
256	16	4.4102 E-1	4.5059 E-1	4.4879 E-1
256	64	4.6435 E-1	4.6833 E-1	4.6758 E-1
256	128	4.5917 E-1	4.7315 E-1	4.7214 E-1
1024	16	4.1001 E-1	3.2198 E-1	3.2171 E-1
1024	64	4.3964 E-1	3.8128 E-1	3.8065 E-1
1024	128	4.4263 E-1	3.9353 E-1	3.9355 E-1

TABLE IX
BIT ERROR RATE ON RAYLEIGH CHANNEL FOR MIMO DETECTION SCHEMES AT SNR 20 DB FOR 1024 OFDM SUBCARRIERS AND 128-QAM FOR 50 NT TO NR

Nr (width × height)	MF	ZF	MMSE
50 (10 × 5)	4.0169 E-1	3.8758 E-1	3.2692 E-1
100 (10 × 10)	3.7667 E-1	7.4001 E-2	7.4057 E-2
200 (10 × 20)	3.5537 E-1	1.4989 E-2	1.4983 E-2
300 (10 × 30)	3.4367 E-1	4.0960 E-3	4.1016 E-3

TABLE X
BIT ERROR RATE ON RICIAN CHANNEL FOR MIMO DETECTION SCHEMES AT SNR 20 DB FOR 1024 OFDM SUBCARRIERS AND 128-QAM FOR 50 NT TO NR

Nr (width × height)	MF	ZF	MMSE
50 (10 × 5)	4.7285 E-1	4.7874 E-1	4.5234 E-1
100 (10 × 10)	4.5919 E-1	3.3164 E-1	3.3132 E-1
200 (10 × 20)	4.6899 E-1	2.4936 E-1	2.4940 E-1
300 (10 × 30)	4.7002 E-1	2.1295 E-1	2.1303 E-1

TABLE XI
BIT ERROR RATE ON CORRELATION CHANNEL FOR MIMO DETECTION SCHEMES AT SNR 20 DB FOR 1024 OFDM SUBCARRIERS AND 128-QAM FOR 50 NT TO NR

Nr (width × height)	MF	ZF	MMSE
50 (10 × 5)	4.0169 E-1	4.9676 E-1	4.7725 E-1
100 (10 × 10)	4.7093 E-1	4.5553 E-1	4.5397 E-1
200 (10 × 20)	4.5018 E-1	4.1148 E-1	4.1102 E-1
300 (10 × 30)	4.4205 E-1	3.7374 E-1	3.7352 E-1

model does not improve with increased SNR. 256 OFDM subcarriers shows a small BER performance improvement, but the largest improvement occurs for 16-QAM, 1024 OFDM subcarriers Rayleigh channel with the MMSE improvement of 1.1702 E-1 at SNR 5 dB down to 7.8125 E-5 at SNR 15 dB (similarly with ZF: 1.1686 E-1 at SNR 5 dB down to 7.8125 E-5 at SNR 15 dB).

Table IX, X and XI show the detailed BER performance for increasing the number of receiver antennas for normal SNR of 20 dB. We see that the performance follows the result of the channel hardening phenomenon where the performance of the channel improves with an increased number of channels, because the fluctuation of the norms of the channels effectively decrease [3]. This follows very closely for Rayleigh channels (best performance increase in ZF and MMSE), however this provides the least performance increase for Correlation channel model. This shows evidence that the channel hardening phenomenon performs best with reducing i.i.d. statistical fluctuations and not correlated channels (although there is still a consistent improvement being made for ZF and MMSE).

III. Conclusion

Least square channel estimation was evaluated on an uplink Massive-MIMO-OFDM system comparing MF, ZF and MMSE detection methods on Rayleigh, Rician and Correlation generated channel models. MMSE detection had the best improved BER performance, only slightly over ZF for a large 50 Nt by 300 Nr MIMO channel, but only making noticeable improvements with increased SNR when the bandwidth of number of OFDM subcarriers was large at 1024 subcarriers for Rayleigh and Rician channels. Despite the Correlation channel having relatively similar MSE of the CSI to Rayleigh channel at high SNR and high OFDM bandwidth, the BER had the worst performance out of all channel models for MMSE and ZF detectors. Future work would suggest that using theoretical models only involving Rayleigh channels will not be sufficient for proper Massive-MIMO detection and investigation should be made to observe the effect of a Massive-MIMO steering matrix. Possible beamforming at the receiver end would improve the BER performance for a Correlation channel if the AoA and AoE between the multiple single antenna users and MIMO system could be estimated. Future work could also investigate non-linear channel estimation and detection methods for improving the MSE of the Rician channel and BER performance of the Correlation channel.

IV. References

[1] S. Yang and L. Hanzo, "Fifty years of MIMO detection: The road to large-scale MIMOs," *IEEE Commun. Surv. Tutorials*, vol. 17, no. 4, pp. 1941–1988, 2015, doi: 10.1109/COMST.2015.2475242.

[2] J. G. Proakis and M. Salehi, *Digital Communications, Fifth Edition*. New York, 2008.

[3] H. Q. Ngo and E. G. Larsson, "No Downlink Pilots are Needed in TDD Massive MIMO," *IEEE Trans. Wirel. Commun.*, vol. 16, no. 5, pp. 2921–2935, Jun. 2016, Accessed: Apr. 08, 2021. [Online]. Available: http://arxiv.org/abs/1606.02348.

[4] E. G. Larsson, O. Edfors, F. Tufvesson, and T. L. Marzetta, "Massive MIMO for next generation wireless systems," *IEEE Commun. Mag.*, vol. 52, no. 2, pp. 186–195, Feb. 2014, doi: 10.1109/MCOM.2014.6736761.

[5] K. Zheng, S. Ou, and X. Yin, "Massive MIMO channel models: A survey," *International Journal of Antennas and Propagation*, vol. 2014. pp. 1–10, 2014, doi: 10.1155/2014/848071.

[6] Y. S. Cho, J. Kim, W. Y. Yang, and C.-G. Kang, *MIMO-OFDM Wireless Communications with MATLAB*, vol. 1, no. 1. John Wiley & Sons, Ltd, 2010.

[7] A. Riadi, M. Boulouird, and M. M. R. Hassani, "Performance of Massive-MIMO OFDM system with M-QAM Modulation based on LS Channel Estimation," *Proc. Int. Conf. Adv. Syst. Emergent Technol. IC_ASET 2019*, no. 1, pp. 74–78, 2019, doi: 10.1109/ASET.2019.8870991.

[8] S. Coleri, M. Ergen, A. Puri, and A. Bahai, "Channel estimation techniques based on pilot arrangement in OFDM systems," *IEEE Trans. Broadcast.*, vol. 48, no. 3, pp. 223–229, 2002, doi: 10.1109/TBC.2002.804034.

[9] M. K. Arti, "A simple scheme of channel estimation in large MIMO systems," *IEEE Veh. Technol. Conf.*, vol. 2016-July, pp. 0–4, 2016, doi: 10.1109/VTCSpring.2016.7504106.

[10] A. Riadi, M. Boulouird, and M. M. Hassani, "Least squares channel estimation of an OFDM massive MIMO system for 5G wireless communications," in *Smart Innovation, Systems and Technologies*, Dec. 2020, vol. 147, pp. 440–450, doi: 10.1007/978-3-030-21009-0_43.

[11] A. Goldsmith, *Wireless Communications*. Cambridge university press, 2005.

[12] "3rd Generation Partnership Project; Technical Specification Group Radio Access Network; Multiple Input Multiple Output Antenna Processing for HSDPA.," *TR 25.876 V1.1.0.* 3GPP, 2002, Accessed: Apr. 12, 2021. [Online]. Available: https://portal.3gpp.org/desktopmodules/Specifications/SpecificationDetails.aspx?specificationId=1309.

[13] H. Yin, D. Gesbert, M. Filippou, and Y. Liu, "A coordinated approach to channel estimation in large-scale multiple-antenna systems," *IEEE J. Sel. Areas Commun.*, vol. 31, no. 2, pp. 264–273, 2013, doi: 10.1109/JSAC.2013.130214.

[14] I. Barhumi, G. Leus, and M. Moonen, "Optimal training design for MIMO OFDM systems in mobile wireless channels," *IEEE Trans. Signal Process.*, vol. 51, no. 6, pp. 1615–1624, 2003, doi: 10.1109/TSP.2003.811243.

[15] M. Cicerone, O. Simeone, and U. Spagnolini, "Channel estimation for MIMO-OFDM systems by modal analysis/filtering," *IEEE Trans. Commun.*, vol. 54, no. 11, pp. 2062–2074, 2006, doi: 10.1109/TCOMM.2006.884849.

[16] B. Trotobas, A. Nafkha, and Y. Louët, "A Review to Massive MIMO Detection Algorithms: Theory and Implementation," in *Advanced Radio Frequency Antennas for Modern Communication and Medical Systems*, IntechOpen, 2020.